ASN NEURO RESEARCH ARTICLE

ASN NEURO 2(5):art:e00048.doi:10.1042/AN20100020

Apotransferrin-induced recovery after hypoxic/ischaemic injury on myelination

Mariano Guardia Clausi, Laura A Pasquini, Eduardo F Soto[1] and Juana M Pasquini[2]

Department of Biological Chemistry and Institute of Chemistry and Biological Physicochemistry (IQUIFIB) and Institute of Investigations of Molecular of Hormonal, Neurodegenerative and Oncologic Diseases (IIMHNO), School of Pharmacy and Biochemistry, University of Buenos Aires-CONICET, Buenos Aires 1113, Argentina

Cite this article as: Guardia Clausi M, Pasquini LA, Soto EF and Pasquini JM (2010) Apotransferrin-induced recovery after hypoxic/ischaemic injury on myelination. ASN NEURO 2(5):art:e00048.doi:10.1042/AN20100020

ABSTRACT

We have previously demonstrated that aTf (apotransferrin) accelerates maturation of OLs (oligodendrocytes) *in vitro* as well as *in vivo*. The purpose of this study is to determine whether aTf plays a functional role in a model of H/I (hypoxia/ischaemia) in the neonatal brain. Twenty-four hours after H/I insult, neonatal rats were intracranially injected with aTf and the effects of this treatment were evaluated in the CC (corpus callosum) as well as the SVZ (subventricular zone) at different time points. Similar to previous studies, the H/I event produced severe demyelination in the CC. Demyelination was accompanied by microglial activation, astrogliosis and iron deposition. Ferritin levels increased together with lipid peroxidation and apoptotic cell death. Histological examination after the H/I event in brain tissue of aTf-treated animals (H/I aTF) revealed a great number of mature OLs repopulating the CC compared with saline-treated animals (H/I S). ApoTf treatment induced a gradual increase in MBP (myelin basic protein) and myelin lipid staining in the CC reaching normal levels after 15 days. Furthermore, significant increase in the number of OPCs (oligodendroglial progenitor cells) was found in the SVZ of aTf-treated brains compared with H/I S. Specifically, there was a rise in cells positive for OPC markers, i.e. PDGFRα and SHH$^+$ cells, with a decrease in cleaved-caspase-3$^+$ cells compared with H/I S. Additionally, neurospheres from aTf-treated rats were bigger in size and produced more O4/MBP$^+$ cells. Our findings indicate a role for aTf as a potential inducer of OLs in neonatal rat brain in acute demyelination caused by H/I and a contribution to the differentiation/maturation of OLs and survival/migration of SVZ progenitors after demyelination *in vivo*.

Key words: Apoptosis, apotransferrin (aTf), hypoxia–ischaemia, myelination, oligodendrogenesis, oligodendroglial differentiation.

INTRODUCTION

We have previously reported that a single intracranial aTf (apotransferrin) injection [ICI (intracranial injection)] to three-day-old rats increases the expression of diverse myelin constituents (Escobar Cabrera et al., 1994; 1997, 2000). We also showed that ICI significantly increased myelin deposition, especially in areas close to the lateral ventricles, using both light and electron microscopy (Marta et al., 2003). The *in vivo* effects of aTf were also reproduced in OL (oligodendrocyte) primary cultures (Paez et al., 2002) as well as in N19 and N20.1 cell lines (Paez et al., 2004). Our results were partially confirmed by other authors who showed that aTF regulates MBP (myelin basic protein) transcription and that its enhancement in myelinogenesis observed in myelin-deficient rats was synergized by EGF-1 (epidermal growth factor 1) (Espinosa de los Monteros et al., 1989, 1999; Espinosa-Jeffrey et al., 2002). Transgenic mice overexpressing the human aTf gene (Saleh et al., 2003) showed an increase in their myelin components similar to that found in rats ICI with aTf. We have also reported that remyelination after cuprizone-induced demyelination in rats is stimulated by aTf (Adamo et al., 2006) and, more recently, we reported that the treatment of iron-deficient animals with a single aTf ICI enhances myelination, improving different biochemical parameters affected by iron deficiency (Badaracco et al., 2008).

White matter damage after H/I (hypoxia/ischaemia) occurs in the immature brain and leads to PVL (periventricular

[1] Eduardo F. Soto deceased on 20 March 2009. Dedicated to Dr Eduardo Soto, an exceptionally devoted and inspiring scientist. His temperance will continue serving as examples to all of us.

[2] To whom correspondence should be addressed (email jpasquin@qb.ffyb.uba.ar).

Abbreviations: aTf, apotransferrin; bHLH, basic helix–loop–helix; BrdU, bromodeoxyuridine; CC, corpus callosum; CL, contralateral; DMEM, Dulbecco's modified Eagle's medium; EGF, epidermal growth factor; FCS, fetal calf serum; GFAP, glial fibrillary acidic protein; H/E, haematoxilin/eosin; H/I, hypoxia/ischaemia; HNE, hydroxynonenal; ICI, intracranial injection/intracranially injected; IL, ipsilateral; IOD, integrated optical density; MBP, myelin basic protein; OL, oligodendrocyte; OPC, oligodendroglial progenitor cell; PBS-T, PBS-0.1% Tween 20; PCNA, proliferating-cell nuclear antigen; PLP, proteolipid protein; PVL, periventricular leukomalacia; RIP, receptor-interacting protein; SVZ, subventricular zone; TfR, transferrin receptor; TUNEL, terminal deoxynucleotidyl transferase-mediated dUTP nick-end labelling.

leukomalacia), a neuropathology associated with brain injury in the premature infant (Volpe, 2001). During the period, infants are at greatest risk for PVL (24–32 post-conceptional weeks), premyelinating OPCs (oligodendroglial progenitor cells) predominate in the human cerebral white matter (Back et al., 2001). Lethal injury to OPCs in the immature (non-myelinated) cerebral white matter was proposed to be a key feature in PVL resulting in hypomyelination (Rice et al., 1981; Volpe, 2001; Rezaie and Dean, 2002; Haynes et al., 2003). Hypomyelination impairs axon conduction, leading to deficit in motor, sensory and/or cognitive function depending on the location of the affected axons. In an effort to reveal the causes for this regeneration failure various researches were focused on the molecular aspects regulating myelination. It is likely that factors involved in normal myelination participate in remyelination of the injured CNS (central nervous system). Molecules implicated in OPC differentiation and maturation might induce positive signals for recovery. aTf is important for normal myelination by acting at several critical steps during OPC development and myelination (Paez et al., 2002, 2004).

The aim of this work is to examine the role of aTf in demyelination and remyelination using a neonatal rat model of white matter damage by H/I as previously described by Vannucci and Vannucci (1997, 2005), and Vannucci et al. (1999). Our results suggest that aTf provides neuroprotection to OPCs after cerebral H/I promoting remyelination of the CC (corpus callosum). Additionally, we have found that aTf treatment increased positive cells for OPC markers and decreased cell death in neonatal SVZ (subventricular zone) subjected to H/I insult. We propose that aTf promotes OPC maturation and myelin recovery in the H/I CC by decreasing iron-mediated toxicity and inducing new OPCs from the SVZ.

MATERIALS AND METHODS

Materials

Human apotransferrin, Höechst 33342, 3,3′ diaminobenzidine, paraformaldehyde, 5-bromo-2-deoxyuridine and Triton X-100 were purchased from Sigma Chemical Co. (Saint Louis, MO, U.S.A.), DMEM (Dulbecco's modified Eagle's medium) F12 was from HyClone (Logan, UT, U.S.A.) and FCS (fetal calf serum) was from Toulbey, Argentina. Recombinant human basic fibroblast growth factor and EGF-1 were from PeproTech (Veracruz, Mexico). DeadEnd™ Colorimetric TUNEL System was purchased from Promega (Madison, WI, U.S.A.). Anti-NG2 antibody and anti-RIP (where RIP is receptor-interacting protein) were purchased from Chemicon (Temecula, CA, U.S.A.). Anti-GFAP (where GFAP is glial fibrillary acidic protein) and anti-Nestin antibodies were purchased from Neuromics (Edina, MN, U.S.A.). Anti-Sonic hedgehog (Shh) was a gift generously given by Dr Andrés Carrasco and anti-PDGFRα was purchased from Santa Cruz Biotechnology (Santa Cruz, CA, U.S.A.). Anti-Nα-acetyllysine-HNE (where HNE is hydroxynonenal) fluorophore antibody was purchased from Calbiochem (Darmstadt, Germany). Anti-cleaved-caspase-3 was purchased from Cell Signalling Technology (Beverly, MA, U.S.A.). *Griffonia simplicifolia* was purchased from Vector Laboratories (Burlingame, CA, U.S.A.). Anti-PCNA (where PCNA is proliferating-cell nuclear antigen) was purchased from Dako Corporation (Copenhagen, Denmark). Anti-CD71 was purchased from PharMingen (San Diego, CA, U.S.A.). Mouse monoclonal antibody to BrdU (bromodeoxyuridine) (5-bromo-2-deoxyuridine) was purchased from Roche (Mannheim, Germany). Anti-β-tubulin III was a gift from Dr Santiago Quiroga (University of Cordoba). Anti-H-ferritin antibody was a gift generously given by J. R. Connor (Pennsylvania State University College of Medicine). Anti-O4 was donated by Dr Ernesto Bongarzone (Cell Biology, University of Illinois in Chicago). Anti-MBP antibody was a gift generously given by Dr A.T. Campagnoni (Mental Retardation Research Center, University of California, Los Angeles, CA, U.S.A.). Anti-CAII antibody was a gift from W. Cammer (A. Einstein College of Medicine, New York, NY, U.S.A.).

Perinatal H/I

Cerebral H/I was produced in 7-day-old Wistar rats (day of birth being postnatal day 1) of either sex by a permanent unilateral common carotid artery ligation followed by systemic hypoxia as described by Rice et al. (1981). Wistar pups of either sex were anaesthetized with ketamine (20 mg/kg body weight) and xylazine (2.5 mg/kg body weight). Once they were fully anaesthetized, a midline neck incision was made; the right common carotid artery was isolated by blunt dissection and then ligated using 5-0 surgical silk. After 3 h recovery, the animals were exposed to 120 min of humidified 8% O_2/92% N_2 at 37°C in a water bath. Control animals were separated from the dam for the same period of time. In our experience, artery ligation failed in two out of ten animals and these rats (without cerebral atrophy) were immediately discarded. A group of animals was ICI in the CC 24 h after H/I with 5 μl of aTf at a concentration of 70 ng/μl (350 ng/brain) under ether anaesthesia. Animals ICI with saline solution were used as controls. The injection was done 3 mm dorsoventral, 0 mm anteroposterior and 0 mm lateral to bregma. All experimental animal instructions were approved by the University of Buenos Aires Committee and animal experimentation was in accordance with the National Institute of Health-Guide for the Care and Use of Laboratory Animals.

Primary neurosphere assay

After 4 days of recovery from H/I, Wistar P11 pups were killed by decapitation and their brains removed using aseptic techniques. The meninges were removed and the region enclosed between the cortex and the ventricles containing the SVZ, under the different experimental conditions, were removed and placed in dishes containing DMEM F12 medium. The SVZ were mechanically minced (three SVZs preparation for each group). After

digestion with trypsin, the cell suspension was passed through a 40 μm Nitex screen and cells were collected by centrifugation at 300 *g* for 5 min. The cells were then plated in 25 cm^2 flasks and kept in DMEM F12 supplemented with B27, 20 ng/ml EGF and 10 ng/ml bFGF-2 (basic fibroblast growth factor 2). To perform neurosphere volumetric measurements, digital photographs were captured from at least 20 neurospheres from each condition after 5 days *in vitro* and volumes were calculated using the Image J software. For the differentiation studies, the neurospheres were dissociated 7 days after plating, and the cells were then plated into poly-ornitine-coated dishes in GDM [glial defined medium (DMEM F12 supplemented with 4 g/l glucose, 2.4 g/l $NaHCO_3$, 25 mg/l insulin, 8 mg/l putrescin, 50 mg/l transferrin, 9.8 μg/l T3, 20 nM progesterone, 8 μg/l selenite and 10 μg/l biotin)] (Casaccia-Bonnefil et al., 1996) without mitogens. After 5 days, the cells were scraped free from their culture dishes using a cell scraper, transferred to flow cytometry tubes and washed with PBS. Subsequently cells were immunostained with a specific antibody O4 (1/50) (3 h at 37°C), followed by fixation with 4% (w/v) paraformaldehyde [1 h at room temperature (25°C)] and incubation overnight with antibody against MBP (1/200) in PBS containing 0.2% bovine serum albumin and 0.03% Triton X-100. The next day, cells were washed with PBS and treated with fluorescent secondary antibodies. To rule out non-specific trapping of antibodies, the cells were incubated in the absence of primary antibodies and in the presence of both secondary antibodies fluorescently labelled (DyLight 488 or 649). The positive fluorescent cells were analysed on a PAS III flow cytometer (Partec, Munich, Germany). The data from 2×10^4 cells were collected, stored and analysed using the FloMax software. To determine the gates and establish background levels, we used the fluorescence in the control tubes.

Cell proliferation and migration

To evaluate cell proliferation and migration, animals of each group were intraperitoneally injected with BrdU (100 mg/kg) 12 h post H/I injury, and saline or aTf injection. Animals were killed three days after H/I (P10). Another group of rats received daily BrdU injections from P8 to P10 and were killed at P21. Coronal sections were analysed for BrdU+ cells using a specific antibody. In these experiments PDGFRα+ cells and CAII were also investigated and their co-localization with BrdU+cells analysed in different experimental conditions.

Sudan Black myelin staining

Floating sections were mounted on to gelatin-precoated glass slides and treated for 5 min with 70% ethanol and immersed in a 70% ethanol solution of 0.5% Sudan Black B for 30 min. Excess staining was removed by washing the slides in 70% ethanol.

Iron staining

Sections were processed using a modification of the Perl's staining instruction to detect ferric iron (Bishop and Robinson, 2001; Moos and Mollgard, 1993). Intensification of Perl's reaction was performed with DAB-Ni sulphate (3′-3′-diaminobenzidine-nickel sulphate; 0.05%:0.01%).

Western-blot analysis

The CC under different experimental conditions were dissected out 2 weeks after H/I (three animals per condition) and placed into tubes containing TOTEX lysis buffer (20 mM Hepes, pH 7.9, 350 mM NaCl, 20% glycerol, 1% Nonidet P40, 1mM $MgCl_2$, 0.5 mM EDTA and 0.1 mM EGTA) (1 ml of buffer per 200 mg tissue). Samples were placed on ice and the tissues homogenized. Tissue was incubated at 95°C for 10 min, and the homogenates centrifuged at 14000 rev./min to remove insoluble material. SVZ tissue was dissected from control, H/I S and H/I aTf hemispheres at P10 (3 SVZs per condition) and homogenized with TOTEX lysis buffer (350 μl buffer per each SVZ). Protein concentration was determined (Bio-Rad Protein Assay kit) and to perform Western blot, 20 and 100 μg of protein sample from CC and SVZ, respectively, were boiled for 5 min in Laemmli buffer containing 4% 2-mercaptoethanol. Proteins were separated by SDS/PAGE using 15% acrylamide–bisacrylamide gels and transferred on to polyvinylidene fluoride membranes. These were blocked in PBS-T (PBS-0.1% Tween 20) containing 5% FCS for 2 h, followed by incubation with primary antibodies overnight at 4°C. The primary antibodies used were anti-MBP (1/1000) in CC samples and anti-Shh (1/200) in SVZ samples. Membranes were washed in PBS-T, incubated for 1 h in horseradishperoxidase-conjugated secondary antibodies diluted 1/2000 in blocking buffer, washed in PBS-T and then developed using 3-3′ diaminobenzidine/Niquel/H_2O_2 mixture. Membranes were stained with Fast Green to evaluate equal protein loading into wells and densitometric analysis was performed using the Gel-Pro analyzer 4.0

Brain section preparation

Animals were anaesthetized with ketamine and xylazine and perfused through the left ventricle of the heart with 30 ml of PBS followed by a 4% solution of paraformaldehyde in PBS. The brains were carefully dissected out and post-fixed in the same solution overnight followed by thorough washing in PBS and cryoprotection in 15 and 30% sucrose in PBS for 24 h. The tissue was then frozen and used for obtaining 40 μm cryostat coronal sections using a Leica CM 1850 cryotome. The floating sections obtained from different areas of the brain were kept in PBS/glycerol (1:1) solution and stored at −20°C until evaluation.

Immunohistochemistry

For immunohistochemistry, floating cryostat sections were rinsed twice with PBS (pH 7.4), then again with PBS/0.1% Triton X-100 (only for cytosolic antigens) and blocked overnight with a solution containing 5% FCS in PBS. For the immunological detection, we performed floating immunohistochemistry. For indirect immunofluorescence, sections were incubated at 4°C with the following antibodies:

anti-NG2 and anti-PDGFRα, both antigens expressed by OLs at early stages of development; anti-Shh, a factor known to induce two bHLH (basic helix–loop–helix) transcription factors (Olig1 and Olig2) that play a key role in the specification of OL precursors; anti-Nestin, a marker of neuroepithelial stem cells; anti-PCNA, to identify proliferating cells; anti-GFAP, to stain astrocytes; anti-H-ferritin to identify iron enriched cells; the biotinylated lectin *G. simplicifolia* (GSA-$1B_4$) for microglial cells; anti-HNE (1/100) to identify free radical peroxidation of lipids; and anti-cleaved-caspase-3 to identify dying cells by apoptosis. We also used antibody against transferrin receptors (CD71) and anti-O4, an antibody for intermediate/late stages of development of OLs (pre-OLs). Identification of mature/adult OLs was carried out using anti MBP, anti-CAII and anti-RIP antibodies. For BrdU immunostaining, sections were pretreated in 2 M HCl for 60 min at 37°C followed by extensive rinses in 0.1 M borate buffer, pH 8.5, and with PBS/0.1% Triton X-100. Afterwards, tissue sections were blocked and incubated with mouse monoclonal anti-BrdU (1/100). After treatment with primary antibodies, sections were rinsed with PBS and incubated for 2 h at room temperature with the appropriate secondary antibody and 5 μM Höechst dye. Sections were rinsed again with PBS, carefully placed on glass slides, dried overnight and mounted with a fluorescence mounting medium for epifluorescence microscopy. Samples were observed under fluorescence or light microscopy in an Olympus BX50 microscope. NG2 and O4/caspase-3 immunostained sections were analysed with a Confocal microscope Eclipse E800 Nikon.

TUNEL (terminal deoxynucleotidyl transferase-mediated dUTP nick-end labelling)

Identification of apoptotic cells by the detection of DNA strand breaks was performed using an *in situ* detection kit (Dead End™ Colorimetric TUNEL system; Promega Corporation, Madison, WI, U.S.A.). As a result of this procedure, which was performed as described by the manufacturer, apoptotic nuclei are stained dark brown.

Image analyses and quantification

Microscope images were carried out with a CoolSnap digital camera and Image J software was used for image analysis. The IOD (integrated optical density) of the fluorescence or number of positive cells per 100 μm^2 was evaluated by measuring 100 μm^2 throughout the area shown by a dotted line in each Figure. Three consecutive sections at the middle dorsal hippocampus were used for quantifications of NG2, CAII, GFAP, GSA-1B4 positive cells and RIP and MBP IOD in the CC. O4 IOD; pyknotic O4 (O4+/caspase3+) and TUNEL-positive cells in the CC were quantified in three consecutive sections at the bregma level. Three consecutive sections at the bregma level were used for quantifications of PCNA, PDGFRα, proliferating OPC (PDGFRα+/BrdU+), GSA-1B4, cleaved-caspase 3 positive cells and Shh IOD in the SVZ. The cell counting results were converted into cells per mm^2 using Abercrombie's correction (Abercrombie, 1946) and the mean value was used for representing one single brain. In one set of assays, the results from experimental groups were normalized by comparison with the results obtained in the control specimens (which were processed in parallel). The control data were set at an arbitrary value of 100% immunoreactivity. The result was expressed as a percentage of its own control. In other set of assays, the results from experimental groups were expressed as the number of positive cells per mm^2.

For measurements of the diameter of the hemispheres, photos from representative H/E (haematoxilin/eosin)-stained sections at P21 were captured by a Exmor R CMOS sensor Camera (DSC-WX1 Sony) connected to a stereo microscope (Leica EZ4) and images were analysed using the Image J software. Diameters of the IL (ipsilateral) and CL (contralateral) hemispheres were measured and the width ratio (WR=IL/CL) determined for each condition.

Statistics

Statistical analysis was performed using GraphPad Prism 4.03 software by analysis of variance followed by Newman–Keuls multiple comparison test. A $P<0.05$ was considered statistically significant. Data are given as the means ± S.E.M.

RESULTS

In this study, only the right carotid artery was ligated. A set of these animals was only ischaemic (so the left hemisphere was used as control), whereas another set, apart from being ischaemic, was submitted to hypoxia. Therefore, in the last case the right brain hemisphere was H/I and the left hemisphere only hypoxic (H). At 24 h post H/I, a group of animals received a single ICI of 350 ng of aTf (hemispheres denominated H/I aTf and H aTf) or saline (hemispheres denominated H/I S and H S). Animals were studied at different time points after H/I insult.

H/I-induced damage on myelination is reversed by ICI of aTf

Brain coronal slices obtained at 3, 8 and 14 days after artery ligation (P10, P15 and P21) were used for CC immunohistochemical studies. Slices were analysed for immunoreactivity using anti-NG2 for identifying immature proliferating OPCs, anti-CNPase (RIP), anti-CAII and O4 to evaluate more differentiated (myelinating) OLs, and anti-MBP to determine myelinated tracts and mature OLs. In turn, Sudan Black staining was used to identify myelin lipids. Immunoreactivity for each of these antibodies was evaluated by measuring the IOD of the reactive cells or the number of positive cells per mm^2, following

the procedure described above. At P21 slices were also analysed using H/E staining for testing the global damage produced by the H/I. At the same age, anti-βIII tubulin was used in order to test neurons from the neocortex as well as their axons.

At P10 a significant increase in NG2+cells (1500 ± 443 versus $311 \pm 55/mm^2$, $P<0.001$) and a 32% decrease in O4+ immunoreactivity ($P<0.01$) was observed in H/I S as compared with the control brain (Figure 1A). It was observed that there was a 1.8-fold decrease in NG2+ cells ($825 \pm 120/mm^2$, $P<0.01$) when aTf was ICI, as compared with the saline-treated H/I group, whereas O4 under the same experimental condition was not completely corrected (Figure 1A).

At P15 a 27% decrease in MBP immunoreactivity was clearly observed in H/I S animals ($P<0.001$), which returned to normal by ICI of aTf ($P<0.05$) (Figure 1B). At P21 RIP immunoreactivity and CAII+ cells as well as myelin lipids evaluated by Sudan Black staining were significantly decreased in H/I S animals as compared with controls (49 and 38% decrease in CAII+ cells and RIP IOD, respectively, in the IL hemisphere; $P<0.001$) (Figures 2A–2D). RIP immunoreactivity returned to control values in H/I when animals were ICI with aTf ($P<0.001$) (Figures 2B, 2C and 2E). When aTf was ICI, CAII+ cells which were diminished in the H S and H/I S hemispheres returned to normal values only in the hypoxic hemisphere ($P<0.001$), whereas in H/I the number of CAII+ cells increased (26% increase as compared with the saline-treated H/I group $P<0.01$) but did not reach normal values (Figures 2D and 2E). At P21, a 38% decrease in MBP immunoreactivity was observed in H/I S animals ($P<0.001$), which returned to normal by ICI of aTf ($P<0.001$; Figures 3A and 3B); these results were further confirmed by Western blot as shown in Figures 3(C) and 3(D).

Global damage after H/I was tested using H/E staining and measuring hemispheric ratios. At P21 there was no difference between both hemispheres in only ischaemic rats (WR= $\sim$1) (Figure 4AI). After H/I, a significant hemisphere difference in the ratio was observed (WR=0.76 ± 0.07, $P<0.001$; Figure 4AII). ApoTf alleviated the extent of IL atrophy (WR= 0.88 ± 0.06; $P<0.01$) (Figure 4AIII). The IL neocortex of H/I animals exhibited reduced numbers of β-tubulin III-positive neurons and axons, whereas when aTf is ICI βIII tubulin immunoreactivity was recovered (Figure 4C).

SVZ and PVWM (periventricular white matter) response post H/I is enhanced in aTf-treated rats

Recent experimental data indicate that diverse forms of ischaemic injury stimulate neural precursor proliferation, particularly from SVZ (Ong et al., 2005; Kadam et al., 2008; Alagappan et al., 2009). In order to test whether aTf induces protection in post-H/I myelination and leads to changes in the SVZ and PVWM response, we investigated the expression of different markers. Nestin positive cells increased in H/I S and H/I aTf rats in the SVZ (Figure 5A). Using another proliferation marker, PCNA, 72 h after H/I, the number of PCNA+ cells were more abundant as compared with control in the SVZ (2.1-fold increase; $P<0.05$). ApoTf treatment induced a further increase in PCNA-positive cells as compared with the H/I S condition (1.7-fold increase; $P<0.01$) (Figures 5B and 5C). The number of PDGFRα+ cells were diminished in H/I S as compared with control (1.7-fold decrease; $P<0.01$). ApoTf prevents this reduction in PDGFRα+ cells ($P<0.01$) (Figures 5D and 5E). To further confirm these results, double labelling of PDGFRα and BrdU was done. The number of PDGFRα+/BrdU+ cells at the SVZ following aTf treatment was 1.7-fold of that in the saline-treated H/I group (Figures 6A and 6B; $P<0.01$). At P21, CAII+/BrdU+ cells were observed in the CC of H/I aTf rats after BrdU injection at P8, P9 and P10 (Figures 6D–6G). As previously described, Shh is an early secreted protein required for OL specification during myelination (Alberta et al., 2001). This morphogen was evaluated 72 h post H/I in the SVZ under different experimental conditions. In coincidence with the results obtained with the expression of PDGFRα, Shh was decreased in animals after H/I injury (52% decrease as compared with control; $P<0.05$) whereas a significant recovery was observed in aTf-treated rats (31% increase as compared with H/I S; $P<0.05$) (Figures 7A and 7B). In agreement with the immunohistochemical results, Western-blot analysis showed a decrease in the non-cleavage form of Shh (present in the cell) in the H/I S condition with a recovery after ICI aTf (Figure 7C). In post H/I, an increase in activated microglia was observed in the SVZ and PVWM area as compared with the control group (7-fold increase; $P<0.001$), with a major increase in H/I aTf rats (12-fold increase; $P<0.01$) (Figures 8B and 8D). TfR (transferrin receptor) expression was also increased after H/I injury, being more evident in H/I aTf rats (Figure 8A). It was found not only in microglial cells but also in some blood vessels as evaluated with GSA-1B4 and Cd71 co-localization (Figures 8C and 8C′).

In addition, apoptosis evaluated by cleaved-caspase-3 in the H/I S SVZ was 18-fold increased as compared with control animals ($P<0.001$). aTf treatment decreased the number of caspase-3 positive cells 8-fold as compared with the saline H/I group (1288 ± 88 versus $160 \pm 67/mm^2$; $P<0.001$) (Figures 9A and 9B). These results suggest that the aTf ICI increases the proliferation of cells committed to the oligodendroglial fate and has a protective effect on the viability of SVZ cells.

In order to further confirm our results in the SVZ, neurospheres generated from control animals, H/I S and H/I aTf at P11 (4 days post H/I) were used for size measurement under the different experimental conditions. The size of spheres was quantified *in vitro* at day 6. In H/I aTf animals, an increase in the neurospheres size was observed (2.8-fold average increase and 7.1-fold average increase in comparison with the control and H/I saline condition respectively) (Figures 10A and 10B). The commitment to OL fate and the differentiation level of OL cells were also evaluated by flow cytometry in neurospheres, which were allowed to differentiate in GDM over 5 days. Increased commitment to the OL fate was observed in ICI aTf post H/I as compared with H/I S animals (1.75-fold versus 1.35-fold increase relative to

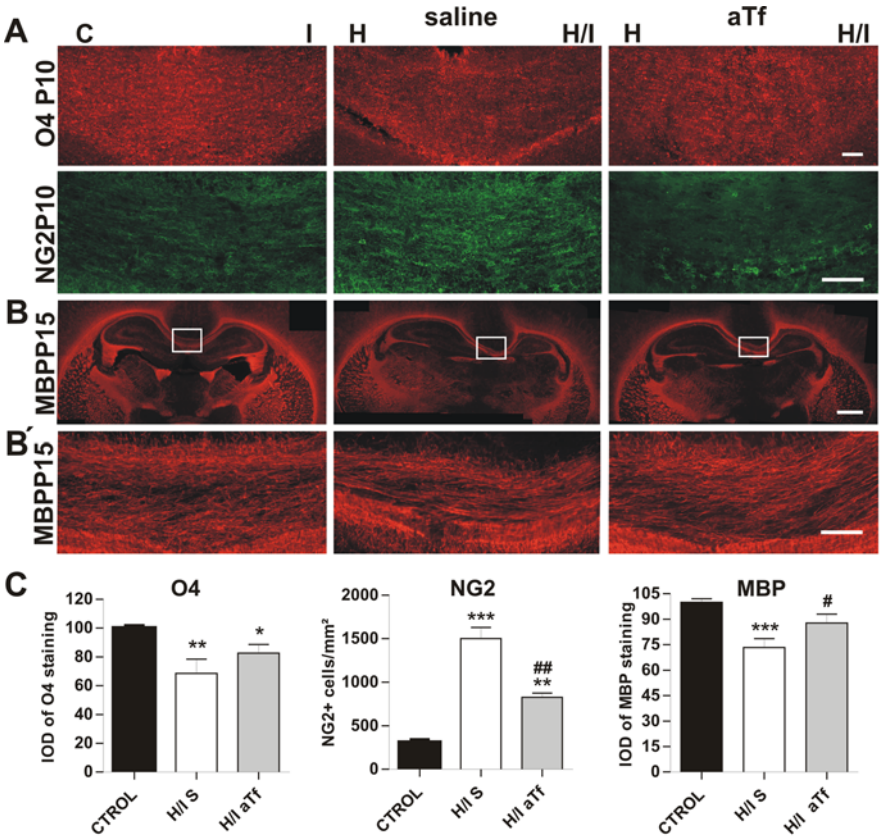

Figure 1 **H/I-induced damage on myelination at P10 and P15 is reversed by ICI of aTf**

Brain coronal sections of control, H/I S and H/I aTf animals at 10 and 15 days of age were stained with antibodies specific for different OLs markers. (**A**) A decrease in O4 and an increase in NG2 immunoreactivity was observed in the CC of H/I S animals as compared with control rats at P10 ($n=9$ H/I S; $n=7$ H/I aTf and $n=6$ Control). (**B**) At P15 the normal MBP staining pattern is altered in H/I S animals and there is a significant recovery in H/I ICI aTf rats ($n=6$ H/I S; 6 H/I aTf and 6 Control). Boxed areas are shown at high magnification. (**C**) O4 and MBP IOD and NG2+ cell/mm^2 were quantified and it was only done in the control and H/I hemispheres. The data show a decrease in O4 and MBP IOD and an increase in NG2+ cell number in H/I S animals and its recovery after the ICI of aTf. Scale bars, 100 μm in (**A**) and (**B**′); 1 mm in (**B**). Values were the means ± S.E.M. of three independent experiments (*$P<0.05$; **$P<0.01$; ***$P<0.001$ relative to C animals; $^{\#}P<0.05$; $^{\#\#}P<0.01$ relative to H/I S animals). C=control; I=ischaemic; H=hypoxic and H/I=hypoxic–ischaemic, S=ICI saline, aTf=ICI of aTf.

control, respectively; $P<0.05$). A higher OL differentiation level was also observed in neurospheres from ICI aTf post-H/I animals as compared with H/I S animals (1.85-fold versus 1.41-fold increase relative to control, respectively; $P<0.05$, Figure 10C).

aTf-induced neuroprotection leads to a decrease in iron, lipid peroxidation and astroglial and microglial activation in CC

Cryostat sections from the brains of the different animal groups were analysed to evaluate astroglial and microglial activation. We used *G. simplicifolia* staining and morphological evaluation to select activated microglia and GFAP as a characteristic marker to identify astrocytes.

H/I induced microglial and astroglial activation. H/I S animals showed increased GFAP immunoreactivity in the CC at P10 (656 ± 402 versus 247 ± 113 cells/mm^2; $P<0.01$) and P15 (630 ± 133 versus 226 ± 163 cells/mm^2; $P<0.001$) as compared with control animals. aTf-treated animals showed a reduction in astroglial activation as compared with the saline H/I group at both P10 (463 ± 86 cells/mm^2; $P<0.05$; Figures 11A and 11C) and P15 (431 ± 187 cells/mm^2; $P<0.05$; Figures 11B and 11C).

As previously reported, H/I increased iron deposition and ferritin expression, which were detected in our experiments at P10 (Figure 12A). ApoTf treatment attenuated iron release in H/I animals at P10 (Figure 12A). When iron levels were evaluated at P15 and P21, we found the same levels of Perl staining in CC of both H/I S and H/I aTf-treated animals, with a slight increase as compared with control rats (data not shown). Concomitantly, ferritin levels always paralleled iron levels (Figure 12A). On the other hand, microglial activation significantly increased in H/I S at P10. The high increase in microglia activation coincided with an iron increase, whereas iron deposits appeared to occur in the microglia (Figure 12B).

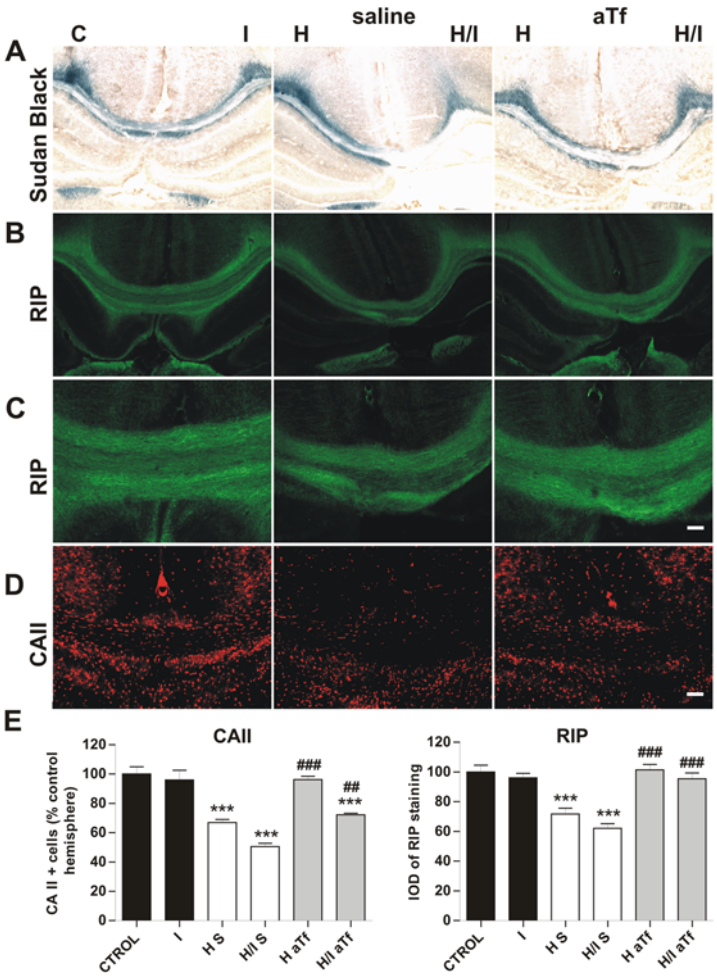

Figure 2 **aTf ICI protects myelination after H/I at P21**

Brain coronal sections of control, H/I S and H/I aTf animals at 21 days of age were stained with Sudan Black and antibodies specific for different OLs markers. (**A**) Sudan Black staining, (**B** and **C**) RIP and (**D**) CAII immunoreactivity. In the IL hemisphere of the H/I S animals a loss of Sudan Black staining and RIP as well as CAII+ cells was observed. All these parameters were significantly recovered in aTf H/I animals. Scale bar, 100 μm in (**C**) and (**D**). (**E**) Values are expressed as IOD (RIP) or number of reactive cells (CAII) and are the means ± S.E.M. of three independent experiments ($n=8$ H/I S; $n=10$ H/I aTf and $n=6$ Control). Quantification was done in all the experimental conditions including I (ischaemic hemisphere) and H (hypoxic hemisphere); $^{***}P<0.001$ relative to C animals; $^{\#\#}P<0.01$; $^{\#\#\#}P<0.001$ relative to H/I S animals. C=control; I=ischaemic; H=hypoxic and H/I=hypoxic–ischaemic, S=ICI saline, aTf=ICI aTf.

The number of GSA-1B4+cells in H/I S was significantly higher than in control (885 ± 229 versus 172 ± 82 cells/mm^2; $P<0.001$) and when aTf was ICI the microglia activation was significantly lower (611 ± 150 cells/mm^2; $P<0.05$) although it was significantly higher than in control rats (Figures 12B and 12C). In order to test whether the decrease in the iron levels in H/I aTf led to a decrease in lipid peroxidation by radical oxygen species, an immunohistochemical analysis using anti-HNE antibody (which recognizes Nα-acetyllysine-HNE fluorophore) a lipid peroxidation product was carried out. At P10, aTf-treated animals showed considerably reduced levels in HNE+ inmunostaining in the IL hemisphere as compared with the H/I S condition (37% decrease; $P<0.05$; Figures 12B and 12C).

aTf reduces the levels of apoptotic cells post H/I in the CC

In order to test the changes in cell survival after H/I, we determined the number of apoptotic cells by TUNEL staining and immunohistochemical studies. TUNEL+ cells were significantly increased in H/I S as compared with control (391 ± 68 versus 17 ± 4/mm^2; $P<0.001$) and significantly reduced when aTf was ICI (52 ± 37 cells/mm; $P<0.001$, Figures 13B and 13D). In order to identify the cells that underwent apoptosis, we carried out co-localization experiments with anti-cleaved-caspase-3 and O4 antibodies as a marker of OLs. Our results showed that a great number of apoptotic cells in the CC were O4+OLs (Figures 13A and 13C).

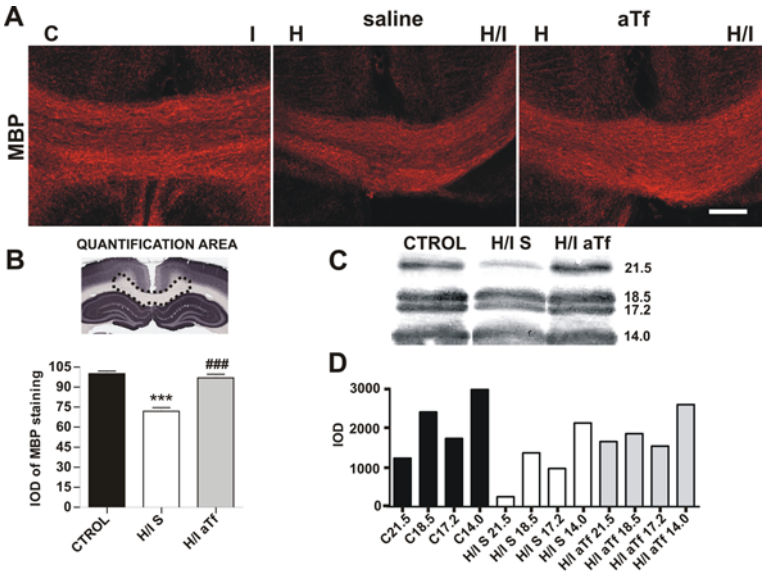

Figure 3 **H/I-induced damage of myelination at P21. MBP in H/I and its reversion by ICI of aTf**

(**A**) Brain coronal sections of control, H/I S and H/I aTf animals at 21 days of age were stained with antibodies specific for MBP resulting lower levels in H/I S and recovered levels in H/I aTf. Scale bar, 100 μm. (**B**) The quantification areas of MBP are shown and was performed as described in the Materials and methods section. Values are expressed as IOD and are the means ± S.E.M. of three independent experiments (n=8 H/I S; n=10 H/I aTf and n=6 Control; ***P<0.001 relative to control animals and $^{###}P$<0.001 relative to H/I S animals). (**C**) Western-blot analysis for the different MBP species using CC lysates from 21-day-old animals. MBP isoforms (21.5, 18.5, 17.2 and 14 kDa) are indicated. (**D**) Western blots were quantified by densitometry and expressed as IOD. Results are from one representative experiment (three animals per condition). C=control; I=ischaemic; H=hypoxic and H/I=hypoxic-ischaemic, S=ICI saline, aTf=ICI aTf.

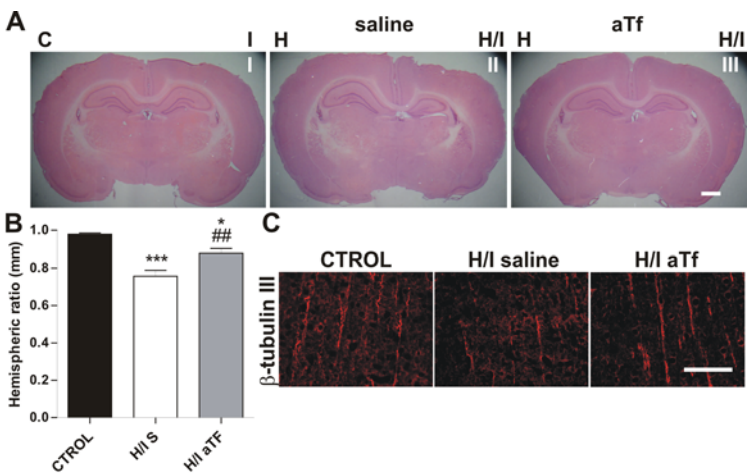

Figure 4 **Neuroprotective effects of aTf against H/I damage**

Brain coronal sections from control, H/I S and H/I aTf at P21 were used throughout. (**A**) Sections of the different experimental conditions were stained with H/E. IL hemispheric atrophy after H/I insult (II) was observed as compared with control (I), whereas treatment with aTf considerably alleviated the atrophy (III). Scale bar, 1 mm. (**B**) Brains were analysed for hemispheric diameter of IL and CL and the WR (IL/CL) calculated for each condition. The results are expressed as the means ± S.E.M. of at least three independent experiments (n=8 H/I S; n=10 H/I aTf and n=6 Control; ***P<0.001; *P<0.05 relative to C animals and $^{##}P$<0.01 relative to H/I S animals). (**C**) Immunoreactivity of β-tubulin III in P21 rats showed that H/I caused neuron and axonal loss in the neocortex which was attenuated by the ICI of aTf. Scale bar, 100 μm. CTROL=control; I=ischaemic; H=hypoxic and H/I=hypoxic-ischaemic, S=ICI saline, aTf=ICI aTf.

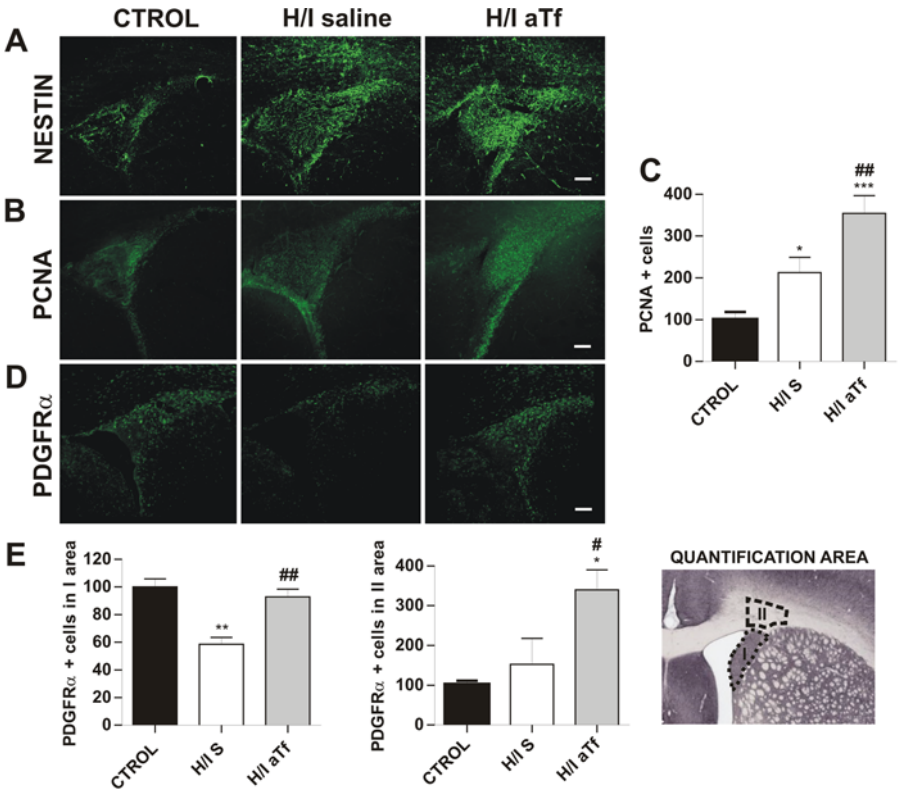

Figure 5 **Nestin, PDGFRα and PCNA immunohistochemistry in the SVZ of the different experimental conditions at P10**
Coronal sections from control, H/I S and H/I aTf were obtained at P10. (**A**) H/I showed an increase in nestin. (**B** and **C**) PCNA+ cells increased 72 h after H/I, and even more in H/I aTf animals. (**D**) PDGFRα+ cells in the IL SVZ were decreased as compared with control animals. Treatment with aTf restored the number of PDGFRα +cells. Scale bar, 100 μm. (**E**) Number of PDGFRα+ cells were quantified in areas highlighted in the Figure with a dotted line. The results in (**C**) and (**E**) are expressed as the % means ± S.E.M. relative to control from at least three independent experiments per condition (n=9 H/I S; n=7 H/I aTf and n=6 Control; *$P<0.05$; **$P<0.01$,***$P<0.001$ relative to C animals; $^{\#}P<0.05$, $^{\#\#}P<0.01$ relative to H/I S animals). CTROL=control, H/I=hypoxic/ischaemic animals, S=ICI saline, aTf=ICI aTf.

DISCUSSION

PVL is one of the major causes of neurological impairment in premature newborns. The aetiology of white matter injury is multifaceted, with H/I being an important underlying factor. Advances in neonatal critical care have dramatically improved survival rates from these injuries, but approx. 50% of H/I infants would subsequently suffer neurologic sequelae. Although selected regions of the brain are damage by H/I at different ages, the white matter peripheral to the lateral ventricles called PVWM is selectively vulnerable to damage in premature infants (Rezaie and Dean, 2002; Johnston, 1997; McQuillen and Ferriero, 2004; Volpe 2003; Follet et al., 2000; Folkerth, 2006).

Since 1994 numerous studies were designed in our laboratory to determine whether aTf has a trophic effect on myelin production independent of iron. It was found that the ICI of a single dose of apoTf (iron-free Tf) in 3-day-old rats produces an increase in the levels of the MBP and CNPase mRNA and protein without affecting those of PLP (proteolipid protein) (Escobar Cabrera et al., 1994, 1997). The effects of aTf were not only specific, but also required the entire molecule, and thus the above-mentioned hypothesis was confirmed when denatured aTf was injected. The mechanism of action of aTf implicating iron could be either direct or indirect. However, when animals were injected with iron dextran at different doses we obtained negative results. Subsequently, it was demonstrated that there was an increase in the mRNA of tubulin and actin, as well as in various microtubule-associated proteins in rat brains receiving ICI with aTf (Cabrera et al., 2000). In congruence with the biochemical studies, morphologic evaluation of apoTf-injected rats showed increased deposition of myelin in the optic nerves and the CC (Marta et al., 2003). All our results were corroborated in transgenic mice with double doses of the human Tf gene developed by Saleh et al. (2003).

The aim of this work was to examine the role of aTf in the remyelination process after a periventricular white matter injury in a rat model of H/I as previously described by Rice et al. (1981). Our results suggest that aTf provides neuroprotection to OPCs after cerebral H/I promoting remyelination in

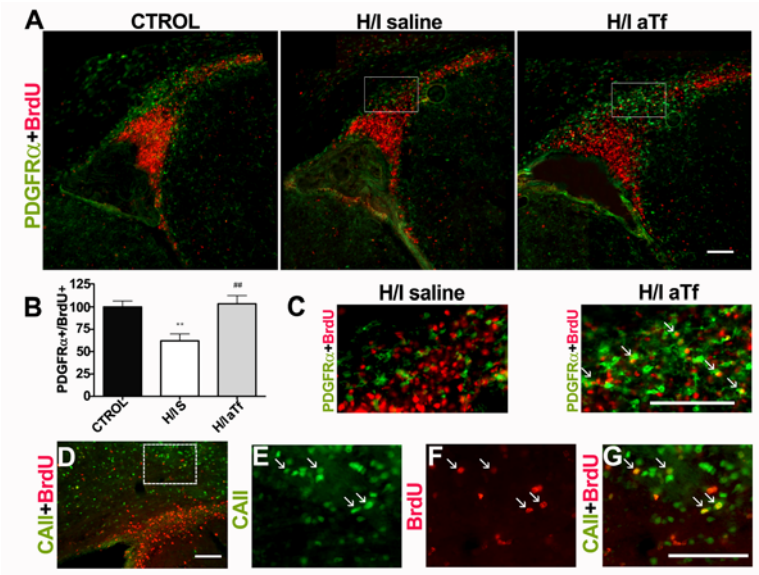

Figure 6 **ICI aTf increases oligodendrogenesis after H/I in the SVZ**
Brain coronal sections from control, H/I S and H/I ICI with aTf were obtained at P10. Animals received a single intraperitoneal BrdU (100 mg/kg) injection 12 h post H/I. (**A**) Sections were stained for PDGFRα and BrdU. (**B**) The number of PDGFRα+/BrdU+ cells/mm^2 was evaluated in the IL SVZ and was the means ± S.E.M. of three independent experiments (n=6 H/I S; n=6 H/I aTf and n=6 control; $^{**}P<0.01$ relative to control animals, $^{\#\#}P<0.01$ relative to H/I S animals). (**C**) High magnification of SVZ of H/I S and H/I ICI aTf as indicated in (**A**). Results showed PDGFRα+ cells co-localizing with BrdU+ (arrows). (**D**) Section from H/I aTf at P21 which received three consecutive BrdU injections (100 mg/kg) from P8 to P10 stained with CAII and BrdU specific antibodies. (**E–G**) High magnifications of the boxed area in (**D**) showing CAII+ cells; BrdU+ cells; and co-localization of CAII and BrdU positive cells, respectively (arrows). Scale bar, 100 μm in (**A**), (**C**), (**D**) and (**G**). CTROL=control, H/I=hypoxic/ischaemic animals, S=ICI saline, aTf=ICI aTf.

different white matter areas and specially the CC. Since association neurons project from the neocortex through the CC, protection by aTf of these neurons was also studied. A strong protection of axons of these neurons was observed probably because of the successful remyelination process aTf mediated. Additionally, we have found that aTf treatment increases proliferation in the SVZ and, as a consequence, the number of positive cells for OPC markers and decreased cell death in neonatal SVZ subjected to H/I insult.

Considerable clinical and experimental data have demonstrated that immature OLs are highly susceptible to H/I insult (Back et al., 2001; 2002). A number of papers have dealt with

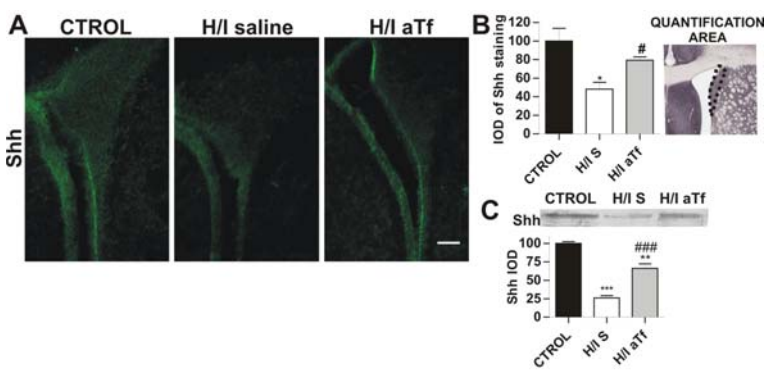

Figure 7 **Shh expression in the SVZ under the different experimental condition**
(**A**) Brain coronal sections from control, H/I S and H/I aTf at P10 were immunostained for Shh. Shh expression in SVZ decreased considerably and became barely detectable in H/I S animals. There is a significant recovery of Shh reactivity in H/I aTf animals. Scale bar, 100 μm. (**B**) Values of Shh IOD in the SVZ were quantified in a highlighted area with a dotted line and were the means ± S.E.M. of three independent experiments (n=9 H/I S; n=7 H/I aTf and n=6 control; $^{*}P<0.05$; $^{***}P<0.001$ relative to C animals; $^{\#}P<0.05$; $^{\#\#\#}P<0.001$ relative to H/I S animals). (**C**) Western-blot analysis of the protein lysates from SVZ at P10 shows decreased non-cleavage Shh expression after H/I S and its recovery after aTf treatment (three animals per condition). CTROL=control, H/I=hypoxic/ischaemic animals, S=ICI saline, aTf=ICI aTf.

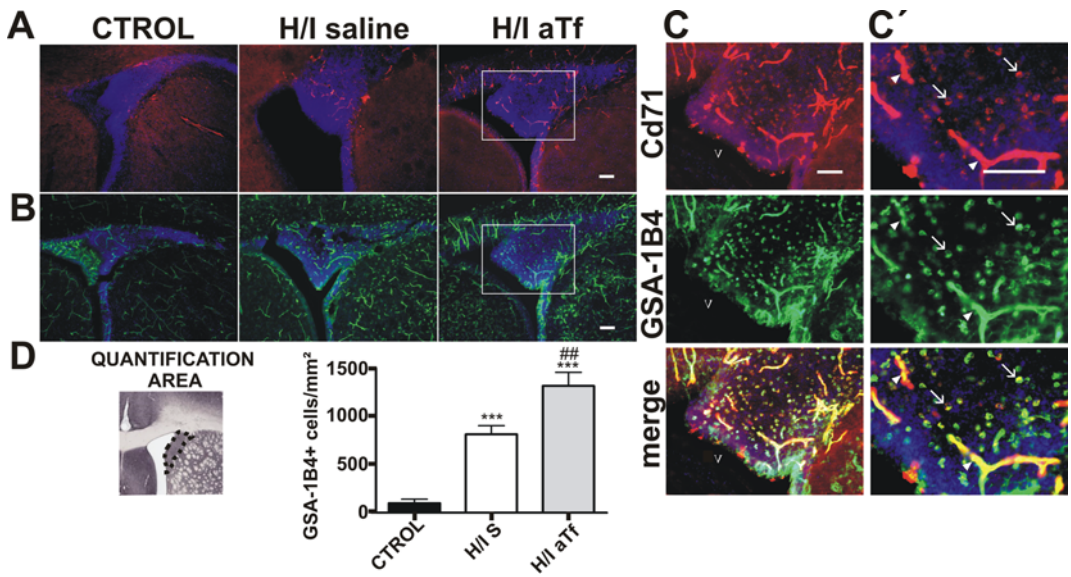

Figure 8 **Microglia and TfR in the SVZ and PVWM in the different experimental conditions at P10**
Brain coronal sections were used throughout. (**A**) TfR expression increases in H/I S as compared with controls with a higher increase in animals ICI with aTf. (**B**) The number of GSA-1B4+ cells are increased in H/I S as compared with controls with a higher increase in animals ICI with aTf. (**C** and **C′**) High magnification of the H/I aTf SVZ (boxed area in panels A and B). Merge shows the distribution of TfR, expression which was found in microglial cells (arrows) and in some blood vessels (arrowheads). Scale bar, 100 μm in (**A–C′**). (**D**) Number of GSA-1B4+ cells/mm^2 were quantified in the SVZ. Results are expressed as the means ± S.E.M. of three independent experiments (n=9 H/I S; n=7 H/I aTf and n=6 control; ***P<0.001; relative to control animals; ##P<0.01 relative to H/I S animals). CTROL=control, H/I=hypoxic/ischaemic animals, S=ICI saline, aTf=ICI of aTf.

this matter and a special mention can be made to that of Back et al. (2006), where they supported the idea that hypoxia inhibits OLs maturation, and that caffeine administration during postnatal development may be useful in the prevention of PVL. On the other hand, intraventricular administration of insulin-like growth factor-1 after H/I rescues OPCs in the perinatal white matter when was given after insult (Wood et al., 2007). The protection of minocycline was associated with its ability to reduce microglial activation. Results of Fan et al. (2006) show that minocycline has long-lasting protective effects in the neonatal rat brain in terms of H/I-brain injury.

In our experiments, animals under H/I showed an increase in immature OLs markers such as NG2 and a decrease in mature OLs evaluated by O4 and MBP, indicating that myelin damage leads to an increased population of OPC. At P10 when aTf was ICI 24 h after H/I injury, the NG2+ cells significantly decreased concomitantly with an increase in O4 and MBP immunostaining, suggesting that aTf induced the differentiation of oligodendroglial precursors formed during injury. The immunoreactivity of O4 could not be completely corrected by ICI of aTf, probably because O4 is a marker not only of mature OLs but also of premyelinating OLs (Back et al., 1998).

An increased TfR expression on the blood vessels and the microglial cells in the PWM after hypoxic injury was reported (Kaur and Ling, 1999). TfRs are involved in the acquisition of iron (Laskey et al., 1988) and it was suggested that microglial cells are involved in the uptake of excessive iron for storage through transferrin receptors (Kaur and Ling, 1999). Although sequestration of excessive iron by microglia in the hypoxic PWM may be a microglia's attempts to protect the immature OLs against its toxic effects, iron accumulation in the PVL may affect the immature OLs directly through oxidative stress, resulting in their death. aTf could help to remove excessive iron by microglial uptake. Moreover, aTf could increase iron uptake, avoiding deleterious effects of free iron.

As already mentioned, results showed that H/I in 7-day-old rats produces severe white matter damage and myelination impairment, as evaluated by different markers of myelinated tracts and oligodendroglial differentiation. These changes were accompanied by augmented iron levels revealed by Perl staining 2 days after H/I reaching a maximum 72 h after injury.

Excitotoxicity, oxidative stress, inflammation and apoptosis are some of the mechanisms involved in the vulnerability of OLs to H/I (Volpe, 2001). It is known that brain iron levels increase after H/I in newborn animals (Adcock et al., 1996) and in turn, excessive iron can contribute to H/I brain damage promoting hydroxyl radical formation (Palmer et al., 1999; Gutteridge, 1992; Paller and Hedlund, 1994) and lipid peroxidation (Yu et al., 2003; Shouman et al., 2008). Activated microglia or astrocytes are the major source of reactive oxygen species that initiate lipid peroxidation by interacting with lipid components of the cellular membranes, resulting in the production of reactive by-products including HNE (Christen, 2000). 4-HNE, a lipid peroxidation product, was also found in the infant brain with PVL (Haynes et al.,

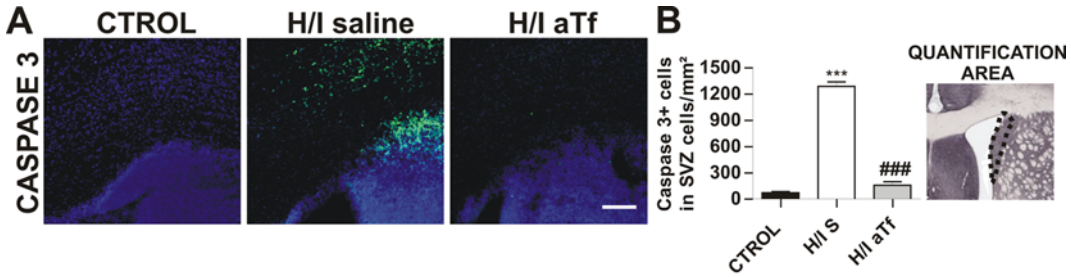

Figure 9 **ICI of aTf reduces the number of apoptotic cells in the SVZ**

(**A**) Brain coronal sections from control, H/I S and H/I aTf at P10 stained with Höechst and immunostained for cleaved-caspase 3. A significant amount of cleaved-caspase 3+ cells were detected in the dorsolateral SVZ after H/I which was reversed when aTf was ICI after H/I. Scale bar, 100 μm. (**B**) Number of cleaved-caspase 3+ cells in the SVZ were quantified in a highlighted area with a dotted line and are the means ± S.E.M. of three independent experiments (n=9 H/I S; n=7 H/I aTf and n=6 control; ***P<0.001 relative to C animals; $^{###}P$<0.001 relative to H/I S animals). CTROL=control, H/I=hypoxic/ischaemic animals, S=ICI saline, aTf=ICI aTf.

2003), indicating the link between PVL and ROS (reactive oxygen species). In a study by Fan et al. (2007), many O4+ OLs in the rat brain have been found double labelled with 4-HNE and malondialdehyde. Our results showed a significant microglial and astroglial activation associated with H/I injury, which was accompanied by an increase in iron deposition and lipid peroxidation. Cells expressing 4-HNE in the CC and in the cingulum 72 h post-H/I insult and the co-localization in O4+ cells with cleaved-caspase-3 immunostaining were found, indicating that O4+ cells might be a susceptible cell population to oxidative stress and apoptotic death after H/I. These alterations were reversed by aTf ICI, thus a reduction in

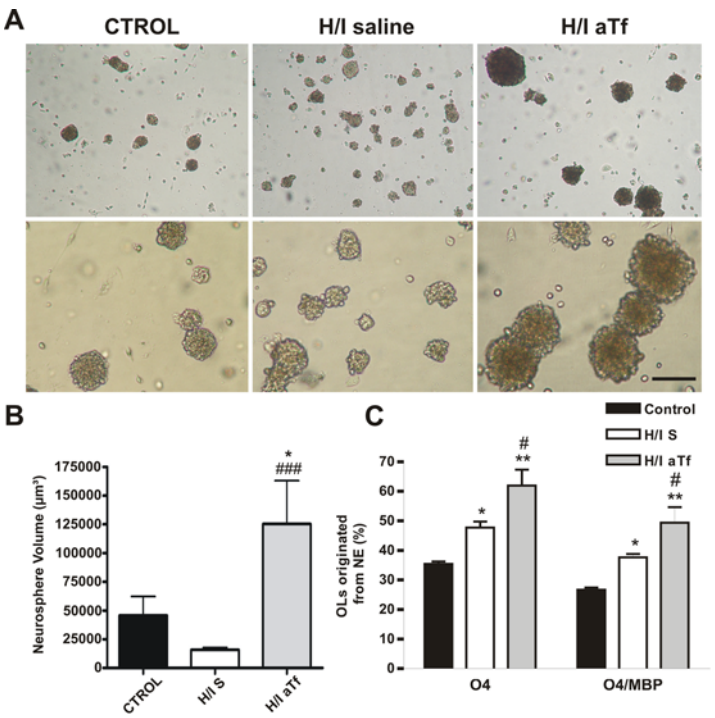

Figure 10 **Neurospheres grow larger when isolated from animals ICI with aTf**

(**A**) Representative phase-contrast photomicrographs of neurospheres generated from SVZ of H/I ICI with saline and aTf. Note the larger size of the spheres in the H/I ICI aTf culture. Scale bar, 100 μm. (**B**) The spheres size was quantified at 6 days *in vitro*. Phase-contrast images of representative neurospheres were captured for quantification. (**C**) Spheres were plated into poly-ornitine-coated dishes and differentiated in growth factor free medium for five days. The differentiated spheres were scrapped, inmunostained for oligodendroglial markers (O4 and MBP) and analysed by flow cytometry. The results are expressed as percentage of O4+ or MBP/O4+ cells of total differentiated cells. Values are from three independent experiment (n=9 H/I S; n=9 H/I aTf and n=6 control; *P<0.05; **P<0.01 relative to C animals; #P<0.05, $^{###}P$<0.001 relative to H/I S animals). CTROL=control, H/I=hypoxic/ischaemic animals, S=ICI saline, aTf=ICI aTf.

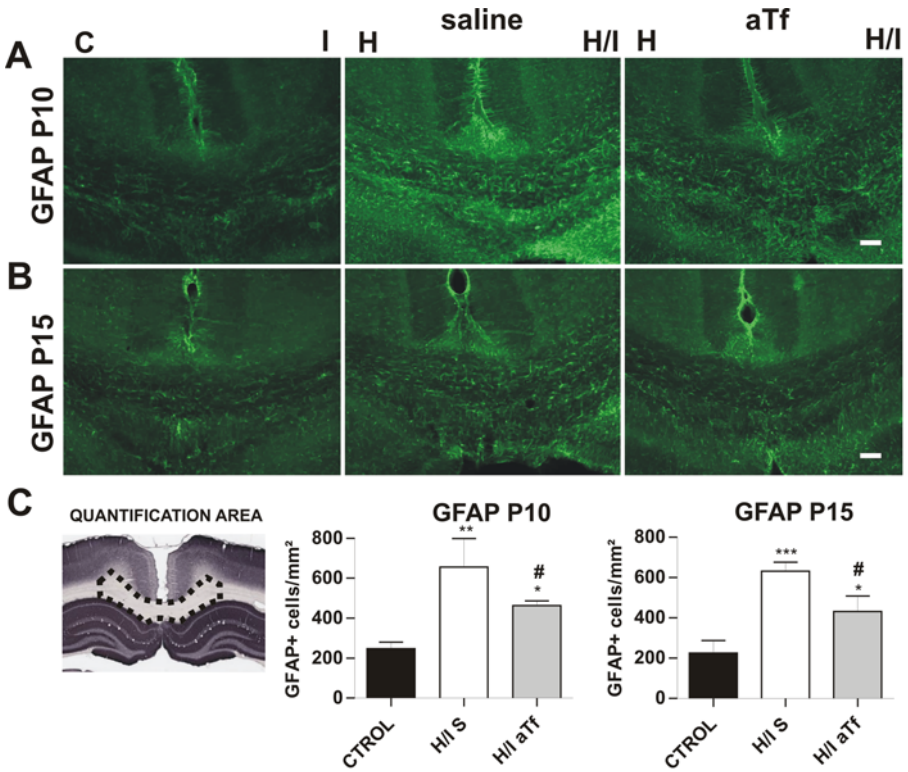

Figure 11 **aTf-induced neuroprotection leads to a decrease in astroglial activation**
Brain coronal sections from control, H/I S and H/I aTf at P10 and P15 were inmunostained for GFAP to identify astrocytes. (**A** and **B**) Exposure to H/I resulted in increased GFAP-positive staining in the CC as compared with control rats at P10 and P15 respectively. ApoTf attenuated H/I-induced astrogliosis at both ages. Scale bar, 100 μm. (**C**) The number of GFAP+ cells was quantified in the highlighted area with a dotted line. The results are expressed as the means ± S.E.M. of three independent experiments (n=6 H/I S; n=6 H/I aTf and n=6 control; *P<0.05; **P<0.01; ***P<0.001; relative to control animals; $^{\#}P$<0.05 relative to H/I S animals). CTROL=control; I=ischaemic; H=hypoxic and H/I=hypoxic–ischaemic, S=ICI saline, aTf=ICI aTf.

iron deposition, free radical generation, lipid peroxidation and apoptotic death of oligodendroglial cells was observed.

We also found increased ferritin expression that paralleled iron accumulation. Cheepsunthorn et al. (1998) reported that the type of ferritin, its cellular distribution and the normal pattern of subcortical white matter myelination are affected by H/I. These authors proposed that the absence of ferritin in OLs prevents them from storing sufficient iron to meet the synthetic and metabolic demands associated with myelination. However, a recent study by Todorich et al. (2009) showed that ferritin and not transferrin is the transporter of iron inside the OLs. In our study, the strong staining by Perl's reaction coincides with the localization of an increased number of microglial cells. Ferritin, probably also augmented in microglia, is capable of transporting iron inside the oligodendroglia, increasing reactive oxygen species generation leading to apoptosis, supported by the observation of cleaved-caspase-3+ cells. Once again, the exogenous aTf ICI has been successfully used to rescue the white matter damage after H/I injury.

There is a growing consensus that the remyelination process is initiated in the SVZ, where OPCs are induced to proliferate, migrate towards demyelinated areas and differentiate into mature myelinating OLs (Picard Riera et al., 2002; Nait-Oumesmar et al., 1999). An increase in the number of neural precursors in the SVZ after moderate ischaemic injuries was observed by Alagappan et al. (2009). These authors also demonstrate that quiescent cells in the SVZ showed an increase in cell division in the presence of the EGFR (epidermal growth factor receptor). Ong et al. (2005) have also studied the effect of H/I injury on SVZ cell proliferation. H/I resulted in enlargement of the IL SVZ at P14–28 and a corresponding increase in BrdU cell number and neurogenesis, based on increased doublecortin immunostaining in the IL SVZ at P14–28. However, 4 weeks after H/I injury in the lesioned striatum, although BrdU/GFAP- and BrdU/RIP-labelled cells were identified, no BrdU/ neuronal nuclear protein double-labelled cells were found. In this study, we observed that H/I injury induced an expansion of the SVZ and an increase in the cell population of progenitors evaluated by the expression of nestin. When aTf was ICI, an enhanced proliferation was demonstrated by the presence of increased PCNA+ cells after aTf injection, with an increase in the amount of PDGFRα +cells, indicating that aTf is capable of not only increasing proliferation but also producing changes in SVZ response,

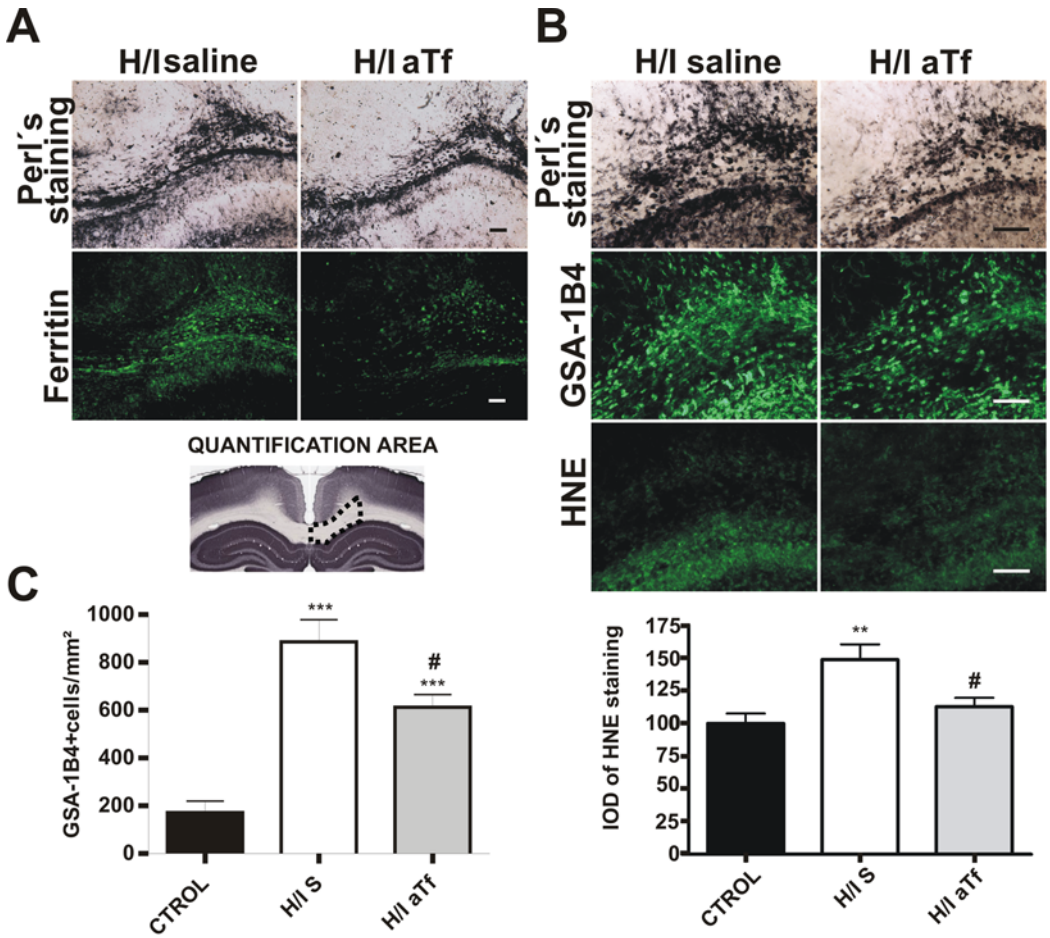

Figure 12 **aTf reduces the levels of iron, lipid peroxidation and microglia activation in H/I; effect of aTf at P10**

Brain coronal sections from control, H/I S and H/I aTf at P10. (**A**) After cerebral H/I, there was a considerable increase in histochemically detectable iron in the IL hemisphere, which was attenuated with aTf treatment. Ferritin expression accompanies the iron levels in the evaluated situations. (**B**) An increased number of microglial cells, as measured by *G. simplicifolia* staining, were detected in the IL CC three days after H/I, coinciding with iron positive cells. An increased lipid peroxidation, evaluated by HNE immunostaining, was also observed in the cingulum area. aTf treatment prevents microglial response and reduces HNE levels. Scale bar, 100 μm in (**A**) and (**B**). (**C**) IOD of HNE and number of GSA-1B4+ cells/mm^2 were evaluated in the quantification area highlighted with a dotted line and are the means ± S.E.M. of three independent experiments (n=9 H/I S; n=7 H/I aTf and n=6 control; ***P<0.001; **P<0.01 relative to control animals; $^{\#}P$<0.05 relative to H/I S animals). CTROL=control, H/I=hypoxic/ischaemic animals, S=ICI saline, aTf=ICI aTf.

converting neural stem cells into oligodendroglial lineage cells. Twelve hours after H/I an intraperitoneal BrdU injection was administered to the animals. When proliferating cells were analysed in the SVZ a higher number of cells already committed to the OLs lineage were observed (BrdU+/PDGFRα+ cells) in animals receiving an ICI of aTf post-H/I as compared with those post-H/I injected with saline.

OL precursors express a number of molecular markers, including *PDGFrα*, PLP/DM20 and the recently cloned bHLH transcription factors, Olig1 and Olig2, which require Shh signalling. An increase in Shh+ immunoreactive cells was detected in the ventricular wall after aTf injection. When this morphogen was tested by Western blot, the protein results paralleled the immunoreactive experiments. These results agree with those previously reported showing that Shh exogenously delivered into the lateral ventricle of adult mice increases the number of proliferating cells expressing the OL marker DM20 in the CC (Loulier et al., 2006). On the other hand, an increase in microglia activation and TfR in the SVZ and PVWM occurs after aTf ICI as compared to the increase observed in H/I, favouring the increase in stem cell/progenitors population by proliferation (Thored et al., 2009), which may also help to remyelinate areas demyelinated by H/I. In concordance with Skoff et al. (2001), we showed an increase in the cleaved-caspase-3+ cells in the SVZ after H/I. These apoptotic cells were not found when aTf was ICI, suggesting that this treatment generates a more favourable environment for the survival of SVZ progenitors.

Our results described in SVZ were strongly supported by those obtained in neurospheres derived from H/I animals ICI

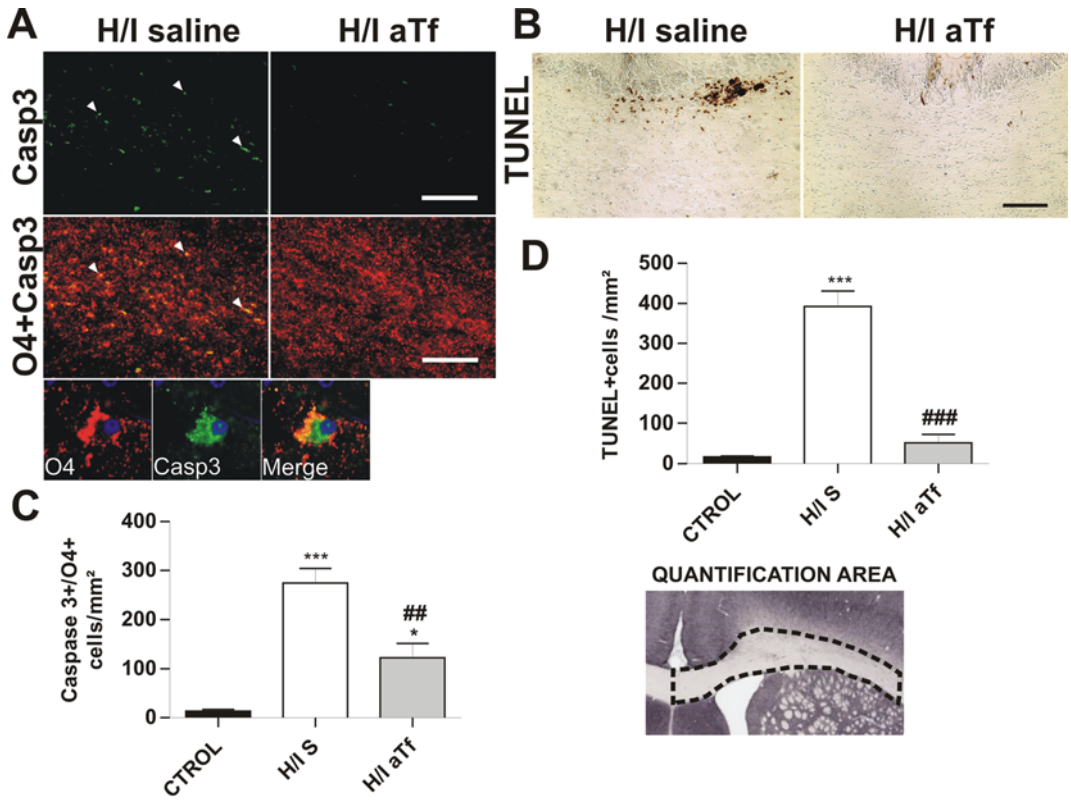

Figure 13 **aTf reduces the number of apoptotic cells post-H/I in CC**

Brain coronal sections from control, H/I S and H/I aTf at P10 were processed for TUNEL and cleaved-caspase 3+ inmunostaining to identify apoptotic cells. (**A**) High levels of cleaved-caspase 3+ cells were observed in the CC of the H/I S animals. Most of these cells co-localized with O4 (arrowheads). When aTf was ICI after H/I, a reduction in the number of cleaved-caspase 3+ cells was observed. High magnification of confocal images of O4+/caspase 3+ cell are also shown. (**B**) An elevated number of TUNEL positive cells, which was reversed by aTf treatment, was also observed in H/I rats. Scale bar, 100 μm in (**A**) and (**B**). (**C**) Cleaved-caspase 3+/O4+ cells were determined and the quantification area is highlighted with a dotted line. The results are expressed as the means ± S.E.M. of at least three independent experiments (n=9 H/I S; n=7 H/I aTf and n=6 control; ***P<0.001; *P<0.05 relative to C animals $^{\#\#}P$<0.01 relative to H/I animals). (**D**) Number of TUNEL-positive cells was evaluated. The results are the means ± S.E.M. of three independent experiments (n=9 H/I; 7 H/I aTf and 6 control; ***P<0.001 relative to control animals; $^{\#\#\#}P$<0.001 relative to H/I S animals). CTROL=control, H/I=hypoxic/ischaemic animals, S=ICI saline, aTf=ICI aTf.

with aTf, which showed an increased commitment to oligodendroglial fate as well as an increase in their size, indicating that aTf is acting on their commitment and also in the differentiation process. Further experiments will be done in order to ascertain whether in our experimental design aTf exerts a direct effect on SVZ response or whether is it mediated by other factors such as microglial activation, Notch receptor modulation and Akt signalling.

To the best of our knowledge, this is the first report on the *in vivo* neuroprotective effect of aTf on OPCs after neonatal cerebral H/I. Our results strongly demonstrated that the aTf treatment after H/I protected myelination through a decrease in iron-induced damage and an accelerated oligodendroglial maturation in the CC. In addition, aTf seemed to increase proliferation and survival of SVZ progenitors and their commitment to oligodendroglial fate. Furthermore, our results suggest that aTf treatment would be a novel therapeutic tool for the recovery after H/I injury. Efforts are being made in our laboratory to develop an aTf molecule capable of permeating the blood brain barrier.

ACKNOWLEDGEMENTS

We acknowledge Dr E. Bongarzone and Dr A. Campagnoni for their gift of O4 and MBP antibodies respectively.

FUNDING

Contract grant sponsor: Agencia Nacional de Promoción de Ciencia y Tecnología PICT no. 38201.

REFERENCES

Abercrombie M (1946) Estimation of nuclear population from microtome sections. Anat Rec 94:239–247.

Adamo AM, Paez PM, Escobar Cabrera OE, Wolfson M, Franco PG, Pasquini JM, Soto EF (2006) Remyelination after cuprizone-induced demyelination in the rat is stimulated by apotransferrin. Exp Neurol 198:519–529.

Adcock LM, Yamashita Y, Goddard-Finegold J, Smith CV (1996) Cerebral hypoxia–ischemia increases microsomal iron in newborn piglets. Metab Brain Dis 11:359–367.

Alagappan D, Lazzarino DA, Felling RJ, Balan M, Kotenko S, Levison SW (2009) Brain injury expands the numbers of neural stem cells progenitors in the SVZ by enhancing their responsiveness to EGF. ASN NEURO 1(2):art:e00009. doi:10.1042/AN20090002.

Alberta JA, Park SK, Mora J, Yuk D, Pawlitzky I, Iannarelli P, Vartanian T, Stiles CD, Rowitch DH (2001) Sonic hedgehog is required during an early phase of oligodendrocyte development in mammalian brain. Mol Cell Neurosci 18:434–441.

Back SA, Craig A, Luo NL, Ren J, Akundi RS, Ribeiro I, Rivkees SA (2006) Protective effects of caffeine on chronic hypoxia-induced perinatal white matter injury. Ann Neurol 60:696–705.

Back SA, Gan X, Li Y, Rosenberg PA, Volpe JJ (1998) Maturation-dependent vulnerability of oligodendrocytes to oxidative stress-induced death by glutathione depletion. J Neurosci 16:6241–6253.

Back SA, Han BH, Luo NL, Chricton CA, Xanthoudakis S, Tam J, Arvin KL, Holtzman DM (2002) Selective vulnerability of late oligodendrocyte progenitors to hypoxia–ischemia. J Neurosci 22:455–463.

Back SA, Luo NL, Borenstein NS, Levine JM, Volpe JJ, Kinney HC (2001) Late oligodendrocyte progenitors coincide with the developmental window of vulnerability for human perinatal white matter injury. J Neurosci 21:1302–1312.

Badaracco ME, Ortiz EH, Soto EF, Pasquini JM (2008) Effect of transferrin on hypomyelination induced by iron deficiency. J Neurosci Res 86:2663–2673.

Bishop GM, Robinson SR (2001) Quantitative analysis of cell death and ferritin expression in response to cortical iron: implications for hypoxia–ischemia and stroke. Brain Res 907:175–187.

Casaccia-Bonnefil P, Aibel L, Chao MV (1996) Central glial and neuronal populations display differential sensitivity to ceramide-dependent cell death. J Neurosci Res 43:382–389.

Cheepsunthorn P, Palmer C, Connor JR (1998) Cellular distribution of ferritin subunits in postnatal rat brain. J Comp Neurol 400:73–86.

Christen Y (2000) Oxidative stress and Alzheimer disease. Am J Clin Nutr 71:621S–629S.

Escobar Cabrera OE, Bongarzone ER, Soto EF, Pasquini JM (1994) Single intracerebral injection of apotransferrin in young rats induces increased myelination. Dev Neurosci 16:248–254.

Escobar Cabrera OE, Soto EF, Pasquini JM (2000) Myelin membranes isolated from rats intracranially injected with apotransferrin are more susceptible to *in vitro* peroxidation. Neurochem Res 25:87–93.

Escobar Cabrera OE, Zakin MM, Soto EF, Pasquini JM (1997) Single intracranial injection of apotransferrin in young rats increases the expression of specific myelin protein mRNA. J Neurosci Res 47:603–608.

Espinosa de los Monteros A, Kumar S, Zhao P, Huang CJ, Nazarian R, Pan T, Scully S, Chang R, de Vellis J. (1999) Transferrin is an essential factor for myelination. Neurochem Res. 24:235–248.

Espinosa de los Monteros A, Pena LA, de Vellis J (1989) Does transferrin have a special role in the nervous system? J Neurosci Res 24:125–136.

Espinosa-Jeffrey A, Kumar S, Zhao PM, Awosika O, Agbo C, Huang A, Chang R, De Vellis J (2002) Transferrin regulates transcription of the MBP gene and its action synergizes with IGF-1 to enhance myelinogenesis in the md rat. Dev Neurosci 24:227–241.

Fan LW, Lin S, Pang Y, Rhodes PG, Cai Z (2006) Minocycline attenuated hypoxia-ischaemia-induced neurological dysfunction and brain injury in the juvenile rat. Eur J Neurosci 24:341–350.

Folkerth ED (2006) Periventricular leukomalacia: overview and recent findings. Pediatr Dev Pathol 9:3–13.

Follett PL, Rosenberg PA, Volpe JJ, Jensen FE (2000) NBQX attenuates excitotoxic injury in developing white matter. J Neurosci 20:9235–9241.

Gutteridge JM (1992) Iron and oxygen radicals in brain. Ann Neurol 32 (Suppl.):S16–S21.

Haynes RL, Folkerth RD, Keefe RJ, Sung I, Swzeda LI, Rosenberg PA, Volpe JJ, Kinney HC. (2003) Nitrosative and oxidative injury to premyelinating oligodendrocytes in periventricular leukomalacia. J Neuropathol Exp Neurol 62:441–450.

Kadam SD, Mulholland JD, Mc Donald JW, Comi AM (2008) Neurogenesis and neuronal commitment following ischemia in a new mouse model for neonatal stroke. Brain Res 1208:35–45.

Kaur C, Ling EA (1999) Increased expression of transferrin receptors and iron in amoeboid microglial cells in postnatal rats following exposure to hypoxia. Neurosci Lett 262:183–186.

Johnston MV (1997) Hypoxic and ischaemic disorders of infants and children. Brain Dev 19:235–239.

Laskey J, Webb I, Schulman HM, Ponka P (1988) Evidence that transferrin supports cell proliferation by supplying iron for DNA synthesis. Exp Cell Res 176:87–95.

Loulier K, Ruat M, Traiffort E (2006) Increase of proliferating oligodendroglial progenitors in the adult mouse brain upon Sonic hedgehog delivery in the lateral ventricle. J Neurochem 98:530–542.

Marta CB, Paez P, Lopez M, Pellegrino de Iraldi A, Soto EF, Pasquini JM (2003) Morphological changes of myelin sheaths in rats intracranially injected with apotransferrin. Neurochem Res 28:101–110.

McQuillen PS, Ferriero DM (2004) Selective vulnerability in the developing central nervous system. Pediatr Neurol 30:227–235.

Moos T, Mollgard K (1993) A sensitive post-DAB enhancement technique for demonstration of iron in the central nervous system. Histochemistry 99:471–475.

Nait-Oumesmar B, Decker L, Lachapelle F Avellana-Adalid V, Bachelin C, Van Evercooren AB (1999) Progenitor cells of the adult mouse subventricular zone proliferate, migrate and differentiate into oligodendrocytes after demyelination. Eur J Neurosci 11:4357–4366.

Ong J, Plane JM, Parent JM, Silverstein FS (2005) Hypoxic–ischemic injury stimulates subventricular zone proliferation and neurogenesis in the neonatal rat. Pediatr Res 58:600–606.

Paez PM, Garcia CI, Davio C, Campagnoni AT, Soto EF, Pasquini JM (2004) Apotransferrin promotes the differentiation of two oligodendroglial cell lines. Glia 46:207–217.

Paez PM, Marta CB, Moreno MB, Soto EF, Pasquini JM (2002) Apotransferrin decreases migration and enhances differentiation of oligodendroglial progenitor cells in an *in vitro* system. Dev Neurosci 24:47–58.

Paller MS, Hedlund BE (1994) Extracellular iron chelators protect kidney cells from hypoxia/reoxygenation. Free Radical Biol Med 17:597–603.

Palmer C, Menzies SL, Roberts RL, Pavlick G, Connor JR (1999) Changes in iron histochemistry after hypoxic–ischemic brain injury in the neonatal rat. J Neurosci Res 56:60–71.

Picard-Riera N, Decker L, Delarasse C, Goude K, Nait-Oumesmar B, Liblau R, Pham-Dinh D, Evercooren AB (2002) Experimental autoimmune encephalomyelitis mobilizes neural progenitors from the subventricular zone to undergo oligodendrogenesis in adult mice. Proc Natl Acad Sci USA 99:13211–13216.

Rezaie P, Dean A (2002) Periventricular leukomalacia, inflammation and white matter lesions within the developing nervous system. Neuropathology 22:106–132.

Rice III JE, Vannucci RC, Brierley JB (1981) The influence of immaturity on hypoxic-ischemic brain damage in the rat. Ann Neurol 9:131–141.

Saleh MC, Espinosa de los Monteros A, de Arriba Zerpa GA, Fontaine I, Piaud O, Djordjijevic D, Baroukh N, Garcia Otin AL, Ortiz E, Lewis S Fiette L, Santambrogio P, Belzung C, Connor JR, de Vellis J, Pasquini JM, Zakin MM, Baron B, Guillou F (2003) Myelination and motor coordination are increased in transferrin transgenic mice. J Neurosci Res 72:587–594.

Shouman BO, Mesbah A, Aly H (2008) Iron metabolism and lipid peroxidation products in infants with hypoxic ischemic encephalopathy. J Perinatol 28:487–491.

Skoff RP, Bessert DA, Barks JD, Song D, Cerghet M, Silverstein FS (2001) Hypoxic–ischemic injury results in acute disruption of myelin gene expression and death of oligodendroglial precursors in neonatal mice. Int J Dev Neurosci 19:197–208.

Thored P, Heldmann U, Gomes-Leal W, Gisler R, Darsalla V, Taneera J, Nygren JM, Jacobsen S-EW, Ekdahl CT, Kokaia Z, Lindvall O (2009) Long-term accumulation of microglia with proneurogenic phenotype concomitant with persistent neurogenesis in adult subventricular zone after stroke. Glia 57:835–849.

Todorich B, Zhang X, Slagle-Webb B, Seaman WE, Connor JR (2009) Tim-2 is the receptor for H-ferritin on oligodendrocytes. J Neuchem 107:1495–1505.

Vannucci RC, Vannucci SJ (1997) A model of perinatal hypoxic ischemic brain damage. Ann N Y Acad Sci 835:234–249.

Vannucci RC, Connor JR, Mauger DT, Palmer C, Smith MB, Towfighi J, Vannucci SJ (1999) Rat model of perinatal hypoxic–ischemic brain damage. J Neurosci Res 55:158–163.

Vannucci RC, Vannucci SJ (2005) Perinatal hypoxic–ischemic brain damage: evolution of an animal model. Dev Neurosci 27:81–86.

Volpe JJ (2001) Neurobiology of periventricular leukomalacia in the premature infant. Pediatr Res 50:553–562.

Volpe JJ (2003) Cerebral white matter injury of the premature infant: more common than you think. Pediatrics 112:176–180.

Yu T, Kui LQ, Ming QZ (2003) Effect of asphyxia on non-protein-bound iron and lipid peroxidation in newborn infants. Dev Med Child Neurol 45:24–27.

Received 18 June 2010/30 September 2010; accepted 18 October 2010

Published as Immediate Publication 20 October 2010, doi 10.1042/AN20100020